Interfacial Choline-Aromatic Cation-Π Interactions Can Contribute As Much To Peripheral Protein Affinity for Membranes as Aromatics Inserted Below the Phosphates

*Qaiser Waheed,[1,2] Hanif M. Khan,[1,2] Tao He,[3] Mary Roberts,[3] Anne Gershenson,[4,5] and Nathalie Reuter[2,6]**

[1] Department of Biological Sciences, University of Bergen, N-5020 Bergen, Norway.

[2] Computational Biology Unit, Department of Informatics, University of Bergen, N-5020 Bergen, Norway.

[3] Department of Chemistry, Boston College, Chestnut Hill, Massachusetts 02467, United States

[4] Department of Biochemistry and Molecular Biology, University of Massachusetts Amherst, Amherst, Massachusetts 01003, United States

[5] Molecular and Cellular Biology Graduate Program, University of Massachusetts Amherst, Amherst, Massachusetts 01003, United States

[6] Department of Chemistry, University of Bergen, N-5020 Bergen, Norway

KEYWORDS. Peripheral proteins, aromatic amino acids, cation-π interactions, membrane affinity, free energy.

ABSTRACT: Membrane binding interfaces of peripheral proteins are restricted to a small part of their exposed surface so the ability to engage in strong selective interactions with membrane lipids at various depths in the interface, both below and above the phosphates, is an advantage. Driven by their hydrophobicity aromatic amino acids preferentially partition into membrane interfaces often below the phosphates. Yet enthalpically favorable interactions with the lipid headgroups, above the phosphate plane, are likely to further stabilize high interfacial positions. Using Free Energy Perturbation we calculate the energetic cost of alanine substitution for 11 interfacial aromatic amino acids from 3 peripheral proteins. We show that involvement in cation-π interactions with the headgroups (i) increases the $\Delta\Delta G_{transfer}$ as compared to insertion at the same depth without cation-π stabilization and (ii) can contribute at least as much as deeper insertion below the phosphates, highlighting the multiple roles of aromatics in peripheral membrane protein affinity.

TOC graphic

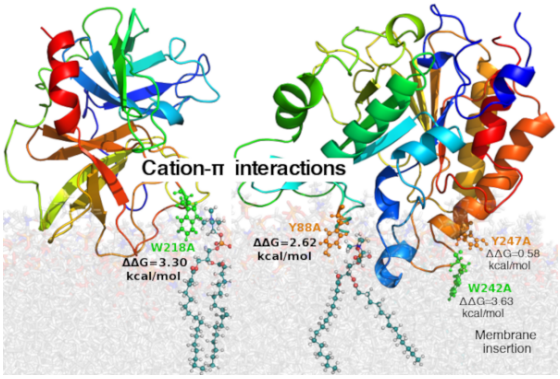

Peripheral membrane proteins populate both soluble and membrane-bound forms.[1] Their membrane-binding mechanism is poorly understood and their membrane-binding regions difficult to distinguish from the rest of their surface.[2] Examples of peripheral membrane proteins include proteins involved in membrane remodeling, lipid transport proteins, enzymes involved in lipid catabolism or phospholipases from snake venoms, to name a few. They often bind specifically to certain lipids and, unlike

transmembrane proteins, peripheral binders cannot rely on a hydrophobic scaffold to attain adequate anchoring depth and tilt angle. Membrane binding interfaces are instead restricted to a small part of their exposed surface and the ability to engage in strong selective favorable interactions with the membrane lipids at various depths is clearly an advantage. The three aromatic amino acids phenylalanine (Phe), tyrosine (Tyr) and tryptophan (Trp) are known to preferentially partition into the complex environment of water/membrane interfaces.[3] Their hydrophobicity explains their preference for membranes over water and their preferential partitioning in membrane interfaces is largely driven by the resulting gain of entropy.[4-7] Moreover favorable interactions with lipid headgroups, such as cation-π interactions[8-12] with the choline groups[13-18], add a favorable enthalpic contribution stabilizing peripheral protein insertion at the upper region of membrane interfaces.[18] Notably, this upper region is the initial site of contact between peripheral proteins and membranes.

Both phosphatidylcholine (PC) and sphingomyelin, the major lipid components of eukaryotic plasma membranes, contain choline groups. We and others have observed cation-π interactions between peripheral proteins and membrane PC lipids (Cf Refs [17, 19-25] and Supporting Information). The energetics of cation-π interactions between various ions and aromatic groups have been estimated mostly in small model systems.[26-29] Yet so far, the energetic contributions of choline-aromatics cation-π interactions to the affinity of proteins for membrane interfaces has not been systematically evaluated and, particularly for Trp and Phe, we lack an estimation of how these interactions compare to simple partitioning of the aromatic groups deeper into the interface.

Molecular dynamics (MD) simulations are particularly useful to access free energy contributions of single amino acids in biomolecular systems.[30-34] We here report free energy perturbation (FEP) calculations of the energetic cost of mutating Phe, Tyr or Trp to alanine in peripheral proteins anchored at the interface of PC lipid bilayers. At equal insertion depth in the interface, the energetic contribution of the aromatics engaging in cation-π interactions is 1.3-2 kcal/mol higher than those not engaging in such interactions.

Notably, the contributions of aromatics involved in cation-π interactions are at least as high as the contribution from those simply inserting deeper into the membrane.

The combination of computations to differentiate cation-pi binders from deeply inserted aromatics, and experiments providing binding affinities are key to this approach. We collected a dataset of aromatic amino acids (4 tyrosines, 4 tryptophans and 3 phenylalanines) from experimentally verified interfacial binding sites of three peripheral proteins which bind to the PC and sphingomyelin rich outer membrane of eukaryotic cells.[19, 21, 35-37] Proteinase 3 (PR3) is a serine protease that binds the surface of human neutrophils.[22, 37-38] *Naja naja atra* phospholipase A_2 (PLA_2) is a fatty acid releasing enzyme from the venom of the cobra snake with broad substrate specificity.[39] *Bacillus thuringiensis* phosphatidylinositol-specific phospholipase C (PI-PLC) is a bacterial hydrolase that targets phosphatidylinositols and binds specifically to PC-rich lipid bilayers. Experimental data using fluorinated tyrosines demonstrate that several of the PI-PLC tyrosines engage in cation-π interactions (Cf SI, Fig.S5 and S6).[40] We ran equilibrium MD simulations for each of the proteins anchored on a pure PC lipid bilayer; the 11 amino acids all insert at the interface and their electron density profiles overlap with that of choline and phosphorus atoms to different extents (Cf Fig.S3), reflecting that they insert at different depths (Cf Table 1). Representative structures were extracted to initiate FEP simulations[41] in order to quantify the contribution of each aromatic amino acid to interfacial binding by mutating it to alanine. The FEP cycle is shown in Fig. 1 with alchemical transformations illustrated along the horizontal directions, at a bilayer and in water: $\Delta G_{MEMB}(\text{Aro} \rightarrow \text{Ala})$ and $\Delta G_{\text{AQ}}(\text{Aro} \rightarrow \text{Ala})$, respectively. The net free energy contribution ($\Delta\Delta G_{transfer}$) for each mutation, obtained by taking the difference between the two (Eq. 1), is reported in Table 1 and Figure 3. The resulting data are directly comparable to experimental binding data for the alanine mutants.[19, 36, 42]

$$\Delta\Delta G_{transfer} = \Delta G_{\text{MEMB}}(\text{Aro} \rightarrow \text{Ala}) - \Delta G_{\text{AQ}}(\text{Aro} \rightarrow \text{Ala}) \qquad = \Delta G_{\text{transfer}}(\text{Aro}) - \Delta G_{\text{transfer}}(\text{Ala}) \qquad (1)$$

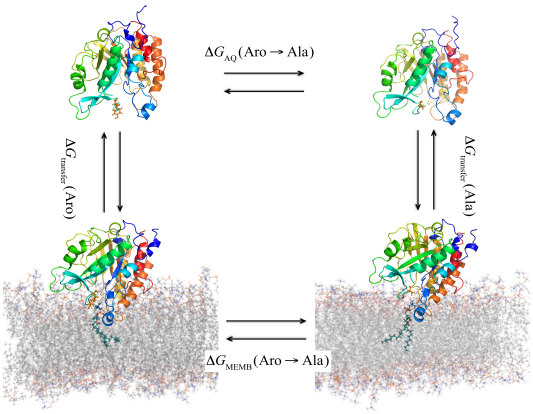

Figure 1. Thermodynamic cycle for FEP calculations. The cycle is illustrated with the substitution of Tyr88 (orange sticks) by alanine in PI-PLC (cartoons) in water and at a DMPC bilayer. The lipid molecule involved in a cation-π interaction with Tyr88 is drawn with balls and sticks.

Table 1. $\Delta\Delta G_{transfer}$ (kcal/mol) for aromatic amino acids in PI-PLC, PLA_2 and PR3.

Aro	Region[a]	Cation-π occupancy (%)[c]	$\Delta\Delta G_{transfer}$(Aro) FEP[d]	Exp[e]
Tyr				
$Y88A_{PI\text{-}PLC}$	III	98.3[28]	2.62	2.7±0.1[19]
$Y246A_{PI\text{-}PLC}$	III	87.3[28]	2.51	3.1±0.6[19]
$Y247A_{PI\text{-}PLC}$	III	16.6[28]	0.58	1.0±0.1[19]
$Y110A_{PLA_2}$	III/IV[b]	39.8	1.36	1.7±0.2[36]
Trp				
$W47A_{PI\text{-}PLC}$	III	0	1.96	2.3±0.4[42]
$W242A_{PI\text{-}PLC}$	II	0	3.63	2.9±0.3[42]
$W61A_{PLA_2}$	III/IV[b]	31.1	2.47	2.9±0.2[36]
$W218A_{PR3}$	III/IV[b]	70.6	3.30	-
Phe				
$F165A_{PR3}$	III	7.1	1.08	-
$F166A_{PR3}$	III	51.8	2.09	-
$F224A_{PR3}$	III	51.9	2.33	-

[a]Region in which the amino acid has its density peak (Fig. S3). [b]Density peak within 2.5 Å of the boundary. [c]Occupancies are given in percentage of the simulation time, values for PI-PLC were taken from Ref[28] and other occupancies were measured over equilibrium simulations (Cf SI). [d]The Bennett Acceptance Ratio estimator[43] yields a statistical error of ±0.15 kcal/mol for each $\Delta\Delta G_{transfer}$ (See Table S2). [e]Experiments were performed with POPC for PI-PLC and DMPC for PLA_2.

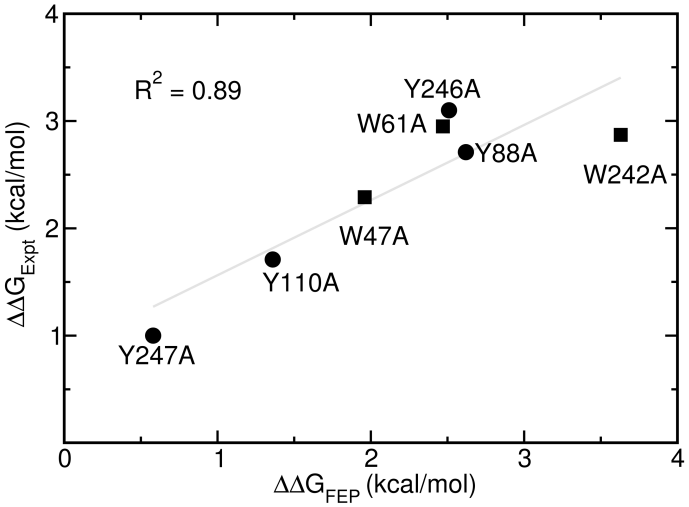

Figure 2. Comparison between computed $\Delta\Delta G_{transfer}$ ($\Delta\Delta G_{FEP}$) and experimentally ($\Delta\Delta G_{Expt}$) determined $\Delta\Delta G_{transfer}$. Experimental values are calculated from the ratio between K_d(mutant) and K_d(WT) on pure PC bilayers.[19, 36, 42]

All values are positive reflecting that the Aro to Ala substitution at the membrane interface comes at a free energy cost. We also report available experimental data: $\Delta\Delta G_{transfer}$ for three tyrosine and two tryptophan residues in PI-PLC calculated from apparent dissociation constants (K_d) of the wild-type (WT) protein and a series of alanine mutants determined primarily using Fluorescence Correlation Spectroscopy (FCS).[19, 42] The experimental values for PLA_2 are calculated in a similar manner from WT and alanine mutants dissociation constants obtained with Surface Plasmon Resonance.[36] Considering the differences in the two approaches and the experimental uncertainties, the FEP results are in very good agreement with the experimental data (Cf Figure 2). Note that the FEP setup is designed to ensure that the calculated $\Delta\Delta G_{transfer}$ (Aro→Ala) corresponds to the specific contribution of the mutated aromatic group to protein lipid interactions at a given insertion depth, which are stable during the FEP calculations. Conversely, the experimental setup consists of two different measurements and depth of insertion may vary as a result of the mutation, local structural differences may also exist experimentally between WT and mutants. The FEP calculations, because they are based on short MD trajectories, purposely limit this possibility.

Using the Wimley-White hydrophobicity scale for proteins at membrane interfaces[44] based on experimentally obtained partition coefficients of short peptides, one can calculate that a tryptophan to alanine substitution comes at a cost of 2 kcal/mol, 1.1 kcal/mol for a Tyr and 1.3 kcal/mol for a Phe. Potential of mean force (PMF) calculations on amino acids analogs from MacCallum et al[34] (Figure 3) indicate an energetic cost of up to 3.6 kcal/mol that depends on the indole insertion depth (dashed purple line). The highest cost is caused by substituting alanine for tryptophan partitioning below the phosphates, in the region where one finds carbonyl groups and the beginning of the tails. This is also the region for which the cost of a Tyr to Ala substitution would be highest (1.79 kcal/mol, green dashed line). The free energy profile is slightly different for phenylalanine (orange line) as the energetically most favorable partitioning of the side chain is 5 Å lower than for Trp and Tyr, with the lipid tails (1.96 kcal/mol). A Phe to Ala substitution in the region where the Tyr and Trp have their preferred partitioning would have a slightly lower cost (1.82 kcal/mol). In what follows we use definitions of interfacial regions II, III and IV from Ref[34] as indicated on Figure 3. In the region of the interface where choline and phosphate groups have their density peaks (region III), $\Delta\Delta G_{transfer}$ are low compared to region II and decrease rapidly with the distance to the center of the bilayer. PMF calculations give about 1.7 kcal/mol for Trp, 1 kcal/mol for Tyr and 0.3 kcal/mol for Phe (values taken in the center of the region).[34] $\Delta\Delta G_{transfer}$ above the phosphate and cholines (region IV) rapidly goes to zero within 5 Å. Our calculated $\Delta\Delta G_{transfer}$ for the aromatics inserted at the interface but not engaging in cation-π interactions are in the expected energy range (empty symbols on Figure 3). Given the slope in region III, and the fact that the symbols represent only the peak of each distribution profiles, discrepancies in this region III are not alarming.

Several of the aromatics in our dataset engage in significant cation-π interactions in regions III and IV. The corresponding calculated $\Delta\Delta G_{transfer}$ values for Tyr and Phe are significantly higher than the PMF values for the aromatics that insert deeper in the interface and are equal to or greater than 2 kcal/mol. For Tyr88 and Tyr246 in PI-PLC we find 2.62 and 2.51 kcal/mol, respectively. Likewise, Phe166 and Phe224

yield $\Delta\Delta G_{transfer}$ of 2.09 and 2.33 kcal/mol, respectively. The values for tryptophan are higher with 3.30 and 2.47 kcal/mol for Trp218 in PR3 and Trp61 in PLA_2, respectively, in agreement with Trp218 of PR3 having a higher cation-π occupancy than Trp61. The values obtained are in the range of the dimerization free energies of tetramethylammonium with indole (3.69 kcal/mol), with phenol (2.26 kcal/mol) and with benzene (2.22 kcal/mol). Together with the agreement with corresponding quantum mechanical computations (3.99, 2.72 and 2.59 kcal/mol,[29] respectively) these results indicate that the computational strategy used and the force field parameters[28-29] perform very well.

Note that the contribution from Trp218 in PR3 and Trp242 in PI-PLC are in the same range even though the peak of Trp218 density profile is located 5 Å above the phosphate plane and that of Trp242 is 5 Å below. The $\Delta\Delta G_{transfer}$ cannot distinguish between deeper insertion in region II and cation-π interactions in region III or IV. For this reason, an Aro/Ala substitution causing an affinity change of 2-3 kcal/mol may easily be interpreted as evidence that the aromatic residue inserts below the phosphate plane in region II. Comparing aromatics that engage in cation-π interactions to those that don't, our calculations indicate that involvement in cation-π interactions in region III increases the $\Delta\Delta G_{transfer}$ from 2 to above 3 kcal/mol for Trp, from 0.6 to 2.5 kcal/mol for Tyr, and from 1.1 to above 2.3 for Phe. The increase upon involvement in cation-π interaction is also true when we compare our $\Delta\Delta G_{transfer}$ values to PMF values[34] or to the Wimley White hydrophobicity scale for interfaces. [44]

If the hydrophobic effect is the driving force for the partitioning of aromatics at membrane interfaces, the deeper an aromatic amino acid can insert the larger the entropy gain. Aromatic amino acids partitioning in regions III and IV thus do not take full advantage of the available entropy gain. It appears from our calculations that cation-π interactions might be providing an enthalpic contribution that at least compensates for the limited entropic gain. The result is that cation-π interactions expand the range of insertion depths at which aromatic amino acids can contribute significantly to membrane binding.

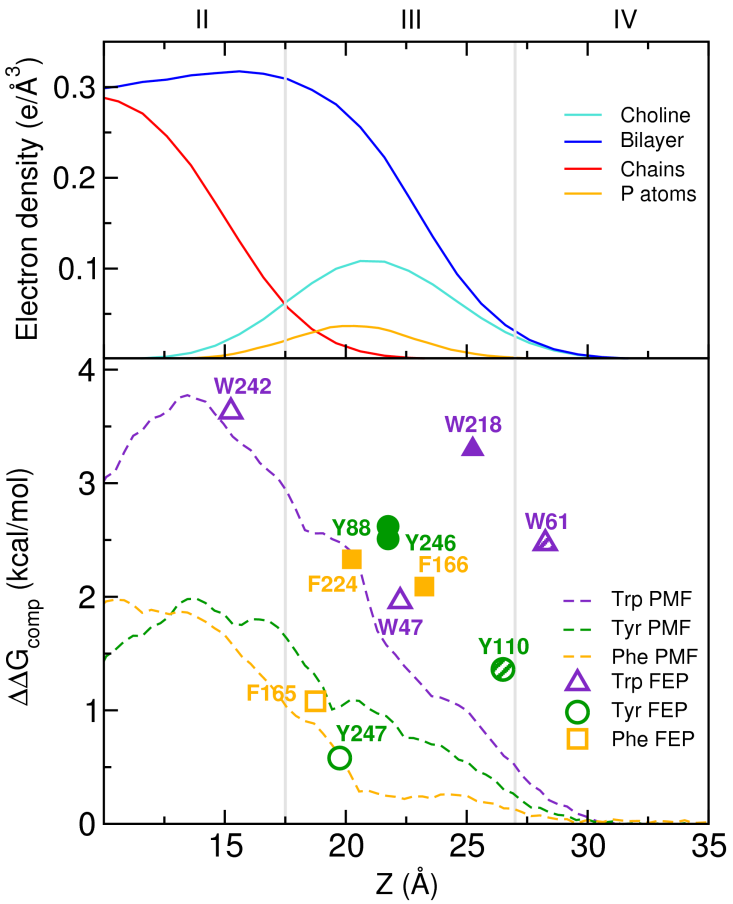

Figure 3. Computed $\Delta\Delta G_{transfer}$ as a function of insertion depth. Z is the distance to the bilayer center. Top: electron density profiles (Cf SI) used for the definition of regions II, III and IV.[34] Bottom: FEP values for Trp (triangles), Tyr (circles) and Phe (squares). Filled symbols: amino acids with cation-π occupancy above 50%; hashed symbols: moderate cation-π occupancy (30-50%); empty symbols: occupancy <30%. PMF values[34] are plotted as dashed lines and reported in Table S1.

Tryptophans engaged in cation-π interactions appear to contribute about 0.5-1 kcal/mol more than tyrosines in similar interactions (Cf. W218 on Fig. 3). One would thus predict that substituting a cation-π interacting tyrosine positioned in the region of the choline headgroups with a tryptophan should provide a significant affinity gain. However, the complexity of interactions between amino acids and lipids at the interface renders such predictions hazardous. We used FCS to measure the affinity of the PI-PLC Y88W variant for POPC small unilamellar vesicles and compared the affinity to that of WT. We chose Tyr88

because we have strong computational and experimental evidence that it engages in long-lasting cation-π interactions with choline headgroups.[19, 35, 40] The K_d increases from 0.016±0.003 mM (WT) to 0.10±0.01 mM (Y88W) corresponding to a $\Delta\Delta G_{transfer}$ of 1.1 kcal/mol, i.e. a loss of affinity reflecting that the tryptophan most likely does not engage in cation-π interactions but instead behaves as Trp47 (Cf. Fig. 3) and is simply inserted in region III. Cation-π interactions with PC are opportunistic and their formation depends on the position and orientation of the aromatic group[28-29, 35] and presumably the local environment.[19-20, 45] This likely explains the lack of strong cation-π interactions for Y88W. This example illustrates the difficulty of predicting energetic contributions or depths of insertion for interfacial aromatic amino acids based simply on affinity data.

Aromatic amino acids involved in cation-π interactions with phosphatidylcholine lipids contribute ca 2.0-2.5 kcal/mol in the case of Phe, 2.5-3.0 kcal/mol for Tyr and 3.0-3.5 kcal/mol for Trp. The contribution of a tryptophan engaged in cation-π interactions above the phosphates is thus at best comparable to its contribution when deeply inserted, i.e. over 3 kcal/mol. For tyrosines and phenylalanines, these interactions appear to be more favorable than inserting below the phosphate plane by 0.5-1 kcal/mol compared to PMF data. It is worth noting that for a transmembrane protein McDonald and Fleming experimentally determined contributions of 3.5 kcal/mol for Trp, and 2.5 kcal/mol for Tyr and Phe at the height of the carbonyl groups where aromatic amino acids have their most favorable energetic contributions.[46] This is 0.5 kcal/mol higher than the PMF predictions for Tyr and Phe and but equal to the PMF value for Trp.

These results provide further support for the hypothesis that aromatic amino acids have multiple roles in membrane binding and interactions. For peripheral proteins with known membrane binding interfaces, FEP calculations provide an experimentally verified, computationally inexpensive way to dissect the roles of particular aromatics in membrane binding, providing insight into protein-membrane interactions and the possibility of engineering specific interaction motifs.

COMPUTATIONAL METHODS

For all systems, the CHARMM-GUI was used to prepare the initial structures (see SI for details).[47-49] All simulations were carried out using NAMD[50] (v. 2.10 and v. 2.12) and the CHARMM36 force field[51-53] with modifications for choline-aromatic cation-π interactions.[28-29] We followed an alchemical route for transforming the aromatic amino acids at the membrane interface to alanine and used the same transformation for the protein solvated in water. This was achieved by performing FEP[41] simulations along the horizontal directions in Figure 1. We performed this transformation both in the forward and backward directions, each consisting of 50 windows and 25 ns-long simulation for every protein-bilayer system and 10 ns divided into 20 windows for the proteins in water. Statistical analyses of the FEP simulations were performed using the Bennett acceptance ratio (BAR) algorithm[43] via the ParseFEP plugin in VMD.[54] The details of equilibrium simulations, FEP simulations and analysis are provided as Supporting Information.

ASSOCIATED CONTENT

Supporting Information

Choline-aromatics cation-π interactions: relevant literature, computational and experimental details, raw free energy data, electron density profiles, simulation snapshots, experimental K_d values. All in one PDF file.

AUTHOR INFORMATION

Corresponding Author

nathalie.reuter@uib.no

All authors have given approval to the final version of the manuscript.

Funding Sources

Research reported in this publication was supported by the Norwegian Research Council (FRIMEDBIO #214167 and FRIMEDBIO #251247 to N.R.) and the National Institute of General Medical Sciences of the National Institutes of Health under award number R01GM060418. QW was supported by the University of Bergen. The computational resources were provided by UNINETT Sigma2 AS, which manages the national infrastructure for high performance computing in Norway.

REFERENCES

1. Monje-Galvan, V.; Klauda, J. B. Peripheral Membrane Proteins: Tying the Knot between Experiment and Computation. *Biochim. Biophys. Acta* **2016,** *1858* (7 Pt B), 1584-93.

2. Fuglebakk, E.; Reuter, N. A Model for Hydrophobic Protrusions on Peripheral Membrane Proteins. *PLoS Comp. Biol.* **2018,** *14* (7), e1006325.

3. von Heijne, G. Membrane Proteins: From Sequence to Structure. *Annu. Rev. Biophys. Biomol. Struct.* **1994,** *23*, 167-92.

4. Fernandez-Vidal, M.; White, S. H.; Ladokhin, A. S. Membrane Partitioning: "Classical" and "Nonclassical" Hydrophobic Effects. *J. Membr. Biol.* **2011,** *239* (1-2), 5-14.

5. Jacobs, R. E.; White, S. H. Mixtures of a Series of Homologous Hydrophobic Peptides with Lipid Bilayers: A Simple Model System for Examining the Protein-Lipid Interface. *Biochemistry* **1986,** *25* (9), 2605-12.

6. Jacobs, R. E.; White, S. H. The Nature of the Hydrophobic Binding of Small Peptides at the Bilayer Interface: Implications for the Insertion of Transbilayer Helices. *Biochemistry* **1989,** *28* (8), 3421-37.

7. Wimley, W. C.; White, S. H. Membrane Partitioning: Distinguishing Bilayer Effects from the Hydrophobic Effect. *Biochemistry* **1993,** *32* (25), 6307-12.

8. Dougherty, D. A. Cation-Π Interactions Involving Aromatic Amino Acids. *J. Nutr.* **2007,** *137* (6 Suppl 1), 1504S-1508S.

9. Dougherty, D. A. The Cation-Π Interaction. *Acc. Chem. Res.* **2013,** *46* (4), 885-93.

10. Mahadevi, A. S.; Sastry, G. N. Cation–Π Interaction: Its Role and Relevance in Chemistry, Biology, and Material Science. *Chem. Rev.* **2013,** *113* (3), 2100-2138.

11. Craven, T. W.; Cho, M.-K.; Traaseth, N. J.; Bonneau, R.; Kirshenbaum, K. A Miniature Protein Stabilized by a Cation–Π Interaction Network. *J. Am. Chem. Soc.* **2016,** *138* (5), 1543-1550.

12. Pletneva, E. V.; Laederach, A. T.; Fulton, D. B.; Kostić, N. M. The Role of Cation–Π Interactions in Biomolecular Association. Design of Peptides Favoring Interactions between Cationic and Aromatic Amino Acid Side Chains. *J. Am. Chem. Soc.* **2001,** *123* (26), 6232-6245.

13. Blaser, G.; Sanderson, J. M.; Wilson, M. R. Free-Energy Relationships for the Interactions of Tryptophan with Phosphocholines. *Org. Biomol. Chem.* **2009,** *7* (24), 5119-28.

14. Dougherty, D. A. Cation-Pi Interactions in Chemistry and Biology: A New View of Benzene, Phe, Tyr, and Trp. *Science* **1996,** *271* (5246), 163-8.

15. Gaede, H. C.; Yau, W. M.; Gawrisch, K. Electrostatic Contributions to Indole-Lipid Interactions. *J. Phys. Chem. B* **2005,** *109* (26), 13014-23.

16. Norman, K. E.; Nymeyer, H. Indole Localization in Lipid Membranes Revealed by Molecular Simulation. *Biophys. J.* **2006,** *91* (6), 2046-54.

17. Petersen, F. N. R.; Jensen, M. Ø.; Nielsen, C. H. Interfacial Tryptophan Residues: A Role for the Cation-Π Effect? *Biophys. J.* **2005,** *89* (6), 3985-3996.

18. Yau, W. M.; Wimley, W. C.; Gawrisch, K.; White, S. H. The Preference of Tryptophan for Membrane Interfaces. *Biochemistry* **1998,** *37* (42), 14713-8.

19. Grauffel, C.; Yang, B.; He, T.; Roberts, M. F.; Gershenson, A.; Reuter, N. Cation−Π Interactions as Lipid-Specific Anchors for Phosphatidylinositol-Specific Phospholipase C. *J. Am. Chem. Soc.* **2013,** *135* (15), 5740-5750.

20. Yang, B.; Pu, M.; Khan, H. M.; Friedman, L.; Reuter, N.; Roberts, M. F.; Gershenson, A. Quantifying Transient Interactions between *Bacillus* Phosphatidylinositol-Specific Phospholipase-C and Phosphatidylcholine-Rich Vesicles. *J. Am. Chem. Soc.* **2015,** *137*, 14-17.

21. Roberts, M. F.; Khan, H. M.; Goldstein, R.; Reuter, N.; Gershenson, A. Search and Subvert: Minimalist Bacterial Phosphatidylinositol-Specific Phospholipase C Enzymes. *Chem. Rev.* **2018,** *118* (18), 8435-8473.

22. Broemstrup, T.; Reuter, N. How Does Proteinase 3 Interact with Lipid Bilayers? *Phys. Chem. Chem. Phys.* **2010,** *12* (27), 7487-7496.

23. Weber, D. K.; Yao, S.; Rojko, N.; Anderluh, G.; Lybrand, T. P.; Downton, M. T.; Wagner, J.; Separovic, F. Characterization of the Lipid-Binding Site of Equinatoxin Ii by Nmr and Molecular Dynamics Simulation. *Biophys. J.* **2015,** *108* (8), 1987-96.

24. Goh, B. C.; Wu, H.; Rynkiewicz, M. J.; Schulten, K.; Seaton, B. A.; McCormack, F. X. Elucidation of Lipid Binding Sites on Lung Surfactant Protein a Using X-Ray Crystallography, Mutagenesis, and Molecular Dynamics Simulations. *Biochemistry* **2016,** *55* (26), 3692-701.

25. Hirano, Y.; Gao, Y. G.; Stephenson, D. J.; Vu, N. T.; Malinina, L.; Simanshu, D. K.; Chalfant, C. E.; Patel, D. J.; Brown, R. E. Structural Basis of Phosphatidylcholine Recognition by the C2-Domain of Cytosolic Phospholipase A2alpha. *eLife* **2019,** *8*.

26. Wheeler, S. E.; Houk, K. N. Substituent Effects in Cation/Π Interactions and Electrostatic Potentials above the Centers of Substituted Benzenes Are Due Primarily to through-Space Effects of the Substituents. *J. Am. Chem. Soc.* **2009,** *131* (9), 3126-3127.

27. Yorita, H.; Otomo, K.; Hiramatsu, H.; Toyama, A.; Miura, T.; Takeuchi, H. Evidence for the Cation–Π Interaction between Cu_2^+ and Tryptophan. *J. Am. Chem. Soc.* **2008,** *130* (46), 15266-15267.

28. Khan, H. M.; Grauffel, C.; Broer, R.; MacKerell, A. D.; Havenith, R. W. A.; Reuter, N. Improving the Force Field Description of Tyrosine–Choline Cation–Π Interactions: Qm Investigation of Phenol–$N(Me)_4^+$ Interactions. *J. Chem. Theory Comput.* **2016,** *12* (11), 5585-5595.

29. Khan, H. M.; MacKerell, A. D.; Reuter, N. Cation-Π Interactions between Methylated Ammonium Groups and Tryptophan in the Charmm36 Additive Force Field. *J. Chem. Theory Comput.* **2019,** *15* (1), 7-12.

30. MacCallum, J. L.; Bennett, W. F.; Tieleman, D. P. Partitioning of Amino Acid Side Chains into Lipid Bilayers: Results from Computer Simulations and Comparison to Experiment. *J. Gen. Physiol.* **2007,** *129* (5), 371-7.

31. Johansson, A. C. V.; Lindahl, E. Position-Resolved Free Energy of Solvation for Amino Acids in Lipid Membranes from Molecular Dynamics Simulations. *Proteins* **2008,** *70* (4), 1332-1344.

32. de Jesus, A. J.; Allen, T. W. The Role of Tryptophan Side Chains in Membrane Protein Anchoring and Hydrophobic Mismatch. *Biochim. Biophys. Acta* **2013,** *1828* (2), 864-76.

33. Gumbart, J.; Roux, B. Determination of Membrane-Insertion Free Energies by Molecular Dynamics Simulations. *Biophys. J.* **2012,** *102* (4), 795-801.

34. MacCallum, J. L.; Bennett, W. F.; Tieleman, D. P. Distribution of Amino Acids in a Lipid Bilayer from Computer Simulations. *Biophys. J.* **2008,** *94* (9), 3393-404.

35. Khan, H. M.; He, T.; Fuglebakk, E.; Grauffel, C.; Yang, B.; Roberts, M. F.; Gershenson, A.; Reuter, N. A Role for Weak Electrostatic Interactions in Peripheral Membrane Protein Binding. *Biophys. J.* **2016,** *110* (6), 1367-1378.

36. Stahelin, R. V.; Cho, W. Differential Roles of Ionic, Aliphatic, and Aromatic Residues in Membrane–Protein Interactions: A Surface Plasmon Resonance Study on Phospholipases A_2. *Biochemistry* **2001,** *40* (15), 4672-4678.

37. Kantari, C.; Millet, A.; Gabillet, J.; Hajjar, E.; Broemstrup, T.; Pluta, P.; Reuter, N.; Witko-Sarsat, V. Molecular Analysis of the Membrane Insertion Domain of Proteinase 3, the Wegener's Autoantigen, in Rbl Cells: Implication for Its Pathogenic Activity. *J. Leukoc. Biol.* **2011,** *90* (5), 941-950.

38. Schillinger, A. S.; Grauffel, C.; Khan, H. M.; Halskau, O.; Reuter, N. Two Homologous Neutrophil Serine Proteases Bind to Popc Vesicles with Different Affinities: When Aromatic Amino Acids Matter. *Biochim. Biophys. Acta* **2014,** *1838* (12), 3191-202.

39. Sumandea, M.; Das, S.; Sumandea, C.; Cho, W. Roles of Aromatic Residues in High Interfacial Activity of *Naja Naja Atra* Phospholipase A_2. *Biochemistry* **1999,** *38* (49), 16290-16297.

40. He, T.; Gershenson, A.; Eyles, S. J.; Lee, Y.-J.; Liu, W. R.; Wang, J.; Gao, J.; Roberts, M. F. Fluorinated Aromatic Amino Acids Distinguish Cation-Π Interactions from Membrane Insertion. *J. Biol. Chem.* **2015,** *290* (31), 19334-19342.

41. Zwanzig, R. W. High-Temperature Equation of State by a Perturbation Method. I. Nonpolar Gases. *J. Chem. Phys.* **1954,** *22* (8), 1420-1426.

42. Feng, J.; Wehbi, H.; Roberts, M. F. Role of Tryptophan Residues in Interfacial Binding of Phosphatidylinositol-Specific Phospholipase C. *J. Biol. Chem.* **2002,** *277* (22), 19867-19875.

43. Bennett, C. H. Efficient Estimation of Free Energy Differences from Monte Carlo Data. *J. Comput. Phys.* **1976,** *22* (2), 245-268.

44. Wimley, W. C.; White, S. H. Experimentally Determined Hydrophobicity Scale for Proteins at Membrane Interfaces. *Nat. Struct. Biol.* **1996,** *3* (10), 842-8.

45. Cheng, J. J.; Goldstein, R.; Gershenson, A.; Stec, B.; Roberts, M. F. The Cation-Π Box Is a Specific Phosphatidylcholine Membrane Targeting Motif. *J. Biol. Chem.* **2013,** *288* (21), 14863-14873.

46. McDonald, S. K.; Fleming, K. G. Aromatic Side Chain Water-to-Lipid Transfer Free Energies Show a Depth Dependence across the Membrane Normal. *J. Am. Chem. Soc.* **2016,** *138* (25), 7946-50.

47. Jo, S.; Kim, T.; Iyer Vidyashankara, G.; Im, W. Charmm-Gui: A Web-Based Graphical User Interface for Charmm. *J. Comput. Chem.* **2008,** *29* (11), 1859-1865.

48. Jo, S.; Lim, J. B.; Klauda, J. B.; Im, W. Charmm-Gui Membrane Builder for Mixed Bilayers and Its Application to Yeast Membranes. *Biophys. J.* **2009,** *97* (1), 50-58.

49. Qi, Y.; Cheng, X.; Lee, J.; Vermaas, Josh V.; Pogorelov, Taras V.; Tajkhorshid, E.; Park, S.; Klauda, Jeffery B.; Im, W. Charmm-Gui Hmmm Builder for Membrane Simulations with the Highly Mobile Membrane-Mimetic Model. *Biophys. J.* **2015,** *109* (10), 2012-2022.

50. Phillips James, C.; Braun, R.; Wang, W.; Gumbart, J.; Tajkhorshid, E.; Villa, E.; Chipot, C.; Skeel Robert, D.; Kalé, L.; Schulten, K. Scalable Molecular Dynamics with Namd. *J. Comput. Chem.* **2005,** *26* (16), 1781-1802.

51. MacKerell, A. D.; Bashford, D.; Bellott, M.; Dunbrack, R. L.; Evanseck, J. D.; Field, M. J.; Fischer, S.; Gao, J.; Guo, H.; Ha, S., et al. All-Atom Empirical Potential for Molecular Modeling and Dynamics Studies of Proteins. *J. Phys. Chem. B* **1998,** *102* (18), 3586-3616.

52. Klauda, J. B.; Venable, R. M.; Freites, J. A.; O'Connor, J. W.; Tobias, D. J.; Mondragon-Ramirez, C.; Vorobyov, I.; MacKerell, A. D.; Pastor, R. W. Update of the Charmm All-Atom Additive Force Field for Lipids: Validation on Six Lipid Types. *J. Phys. Chem. B* **2010,** *114* (23), 7830-7843.

53. Best, R. B.; Zhu, X.; Shim, J.; Lopes, P. E. M.; Mittal, J.; Feig, M.; MacKerell, A. D. Optimization of the Additive Charmm All-Atom Protein Force Field Targeting Improved Sampling of the Backbone Φ, Ψ and Side-Chain X1 and X2 Dihedral Angles. *J. Chem. Theory Comput.* **2012,** *8* (9), 3257-3273.

54. Liu, P.; Dehez, F.; Cai, W.; Chipot, C. A Toolkit for the Analysis of Free-Energy Perturbation Calculations. *J. Chem. Theory Comput.* **2012,** *8* (8), 2606-2616.